Estimating uveal melanoma volume with ellipsoid tumour models

Klaassen, L.; Ferreira, T.A.; Luyten, G.; Beenakker, J.W.M.

Received: 6 November 2024 | Accepted: 23 March 2025

DOI: 10.1111/aos.17492

Acta Ophthalmologica

ORIGINAL ARTICLE

Estimating uveal melanoma volume with ellipsoid tumour models

Lisa Klaassen[1,2,3,4] | **Teresa A. Ferreira**[2] | **Gregorius Luyten**[1] | **Jan-Willem M. Beenakker**[1,2,3,4]

[1]Department of Ophthalmology, Leiden University Medical Center, Leiden, the Netherlands

[2]Department of Radiology, Leiden University Medical Center, Leiden, the Netherlands

[3]Department of Radiation Oncology, Leiden University Medical Center, Leiden, the Netherlands

[4]HollandPTC, Delft, the Netherlands

Correspondence
Lisa Klaassen, postal zone J3-S, P.O. Box 9600, 2300 RC Leiden, the Netherlands.
Email: l.klaassen@lumc.nl

Funding information
Varian Medical Systems, Grant/Award Number: 2020016

Abstract

Purpose: Ellipsoid tumour models are used to approximate the tumour volume of uveal melanomas, as the conventionally used ultrasound does not provide a three-dimensional visualization of the tumour. However, these models are a simplification of the actual tumour geometry. The aim of this study was to determine to what extent several of these frequently used ellipsoid tumour models accurately describe uveal melanoma volume.

Methods: Tumours were delineated on contrast-enhanced T1-weighted MRI for 70 uveal melanoma patients. The MRI-delineated volume was compared with three ellipsoid models, which used two-dimensional measurements such as thickness and basal diameters as input: half ellipsoids with round ($V_{roundbase}$) or oval base ($V_{ovalbase}$) and a paraboloid consisting of two parts, also incorporating the curvature of the eye wall ($V_{twoparts}$).

Results: Statistically significant relative differences between MRI-delineated and model volume of 53±32% ($V_{roundbase}$), 26±24% ($V_{ovalbase}$) and 15±24% ($V_{twoparts}$) were observed ($p<0.001$). Tumour volume and shape did not influence the difference between the model volumes and MRI-delineated tumour volume.

Conclusion: All tumour models result in considerable systematic overestimations of tumour volume, with large variations in overestimation between patients. Adding the perpendicular basal diameter to the model decreases this variation. Although ellipsoid tumour models have been shown to be valuable on a group level, they should be used with caution for individual patients.

KEYWORDS
MRI, prognosis, uveal melanoma, volume

1 | INTRODUCTION

Uveal melanoma, although the most frequently occurring primary ocular malignancy in adults, is a rare disease with an incidence of about 2–10 per million per year, varying per region (Hou et al., 2024; Jager et al., 2020; Wu et al., 2023). Despite the high local control after treatment of the primary tumour (Buonanno et al., 2022; Marinkovic et al., 2021; Mishra & Daftari, 2016), 5-year survival is still relatively poor at 25%–97% (Force, 2015), depending on clinical, histopathological and genetic factors. As prognosis is important for patient counselling, several methods have been described to non-invasively estimate prognosis or metastatic risk, including tumour size (Kaliki et al., 2015). Shields et al. (2009) described a 5% increase in the 10-year risk of metastasis at each millimetre increase of tumour thickness. In another study, increasing basal diameter was associated with lower survival (Kujala et al., 2003). These two tumour measurements are complemented with factors such as ciliary body involvement in the frequently used AJCC TNM staging system (Force, 2015; Kivelä et al., 2016). Furthermore, tumour volume has been described to be a better prognostic factor (Char et al., 1997; Gass, 1985; Hagstrom et al., 2024; Li et al., 2003; Richtig et al., 2004; Stalhammar et al., 2024).

However, with conventional ophthalmic imaging methods, such as ultrasound, fundoscopy or optical coherence tomography, tumour volume cannot be measured (Solnik et al., 2022). Several studies, therefore, propose tumour models using two-dimensional measurements, such as thickness and diameter, to estimate tumour volume. For

example, Richtig et al. (2004) proposed a half-ellipsoid model in which the tumour thickness and largest basal diameter are used. Other studies added more measurements to further personalise these tumour models, such as the perpendicular basal diameter (Char et al., 1997; Gass, 1985) or eye diameter (Li et al., 2003).

These studies assume that uveal melanomas can be described as a regularly shaped ellipsoid. However, several studies show that uveal melanomas not only appear in the common dome shape, but also in bilobated, overhanging or mushroom configurations (Ferreira et al., 2022; Foti et al., 2021; Jaarsma-Coes, Ferreira, Marinkovic, et al., 2023). Therefore, the aforementioned ellipsoid tumour models are a simplification of tumour geometry and may therefore not be accurate, influencing prognosis estimation.

With the introduction of ocular MRI in the clinical care of uveal melanoma patients, a non-invasive method of three-dimensional tumour imaging has become available (Foti et al., 2021; Jaarsma-Coes, Klaassen, Marinkovic, et al., 2023; Solnik et al., 2022). High-resolution sequences enable more accurate methods for measuring tumour thickness, diameters and clip-tumour distances than conventional ophthalmic imaging has been able to (Ferreira et al., 2019, 2022; Jaarsma-Coes, Ferreira, Marinkovic, et al., 2023; Klaassen et al., 2022). Furthermore, isotropic sequences enable three-dimensional (3D) tumour delineations (Daftari et al., 2005; Jaarsma-Coes, Klaassen, Verbist, et al., 2023).

The aim of this study was to determine to what extent several frequently used ellipsoid tumour models can approximate uveal melanoma volume measured on MRI.

2 | METHODS

2.1 | Patient population

For this study, data from two existing cohorts were analysed retrospectively.

For the first cohort, all UM patients who received an MRI between May 2019 and March 2021 as part of clinical care or in the context of a scientific study were evaluated retrospectively. Patients in this cohort with tumours with a thickness below 7 mm were generally treated with ^{106}Ru brachytherapy (apex dose 130 GyE), whereas larger tumours and juxtapapillary tumours were treated with proton beam therapy (tumour dose 60 GyRBE) or enucleation (Marinkovic et al., 2016, 2021). Patients from this cohort were included if they had a primary tumour without extrascleral extension. Patients for whom the tumour extent could not be assessed accurately on MRI, according to the report of a neuroradiologist with over 20 years of experience, were excluded. Furthermore, for patients who underwent tumour endoresection after primary treatment, the scan after treatment was excluded.

The second cohort consisted of 14 patients who underwent MRI scans before proton beam therapy in the context of a separate prospective scientific study between November 2022 and February 2024.

Both studies were conducted after approval of the local ethics committee (METC Leiden-Den Haag-Delft, NL73433.058.20 and NL57130.058.16), in accordance with the Declaration of Helsinki.

2.2 | MRI acquisition and analysis

Tumours were delineated on the 3D contrast-enhanced T1-weighted scans (Figure 1), with the 3D non-contrast-enhanced T1-weighted scan and 3D T2-weighted scans used as a reference to distinguish tumour from surrounding structures. These MRI scans were acquired with a 3 tesla MRI scanner (Ingenia Elition, Philips Healthcare, the Netherlands) with a 4.7 cm surface receive coil (Philips Healthcare), using an earlier described protocol (Ferreira et al., 2019, 2022). The MRI scans had an acquisition voxel size of $0.8 \times 0.8 \times 0.8\,mm^3$ and a reconstruction voxel size of $0.4 \times 0.4 \times 0.4\,mm^3$, and the contrast-enhanced T1-weighted scan was acquired in 2 minutes and 7 seconds.

Tumour delineation was performed by one observer (LK), and the contours were verified and, if necessary, corrected by an ophthalmic MRI expert (JWB) with 10+ years of experience, based on the clinical evaluation by a neuroradiologist with over 20 years of experience.

Tumour thickness, largest basal diameter (LBD) and perpendicular basal diameter (PBD) were computed automatically based on the 3D tumour contours according to a previously published method (Klaassen et al., 2022). These MRI measurements were used as inputs for the tumour models.

Tumour shape was assessed visually and classified as regular (dome-shaped or flat lesions) or irregular (mushroom-shaped or bilobated lesions). In general, tumour shape was taken from the radiology report. Tumours for which the shape was not mentioned in the radiology report were independently assessed by two

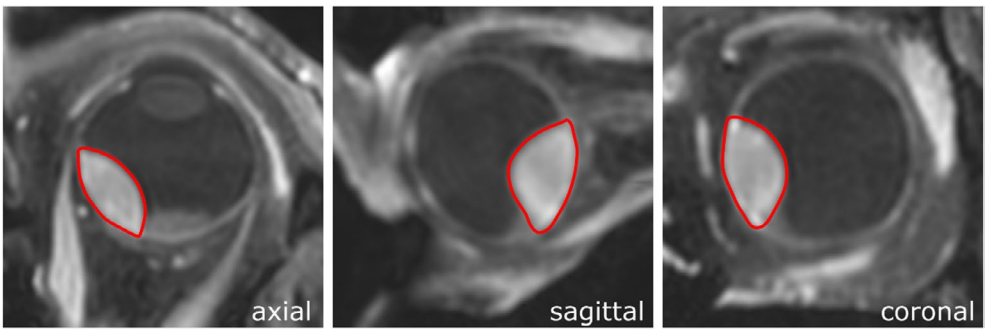

FIGURE 1 Tumour delineation (red contour) was performed on 3D contrast-enhanced T1-weighted MRI.

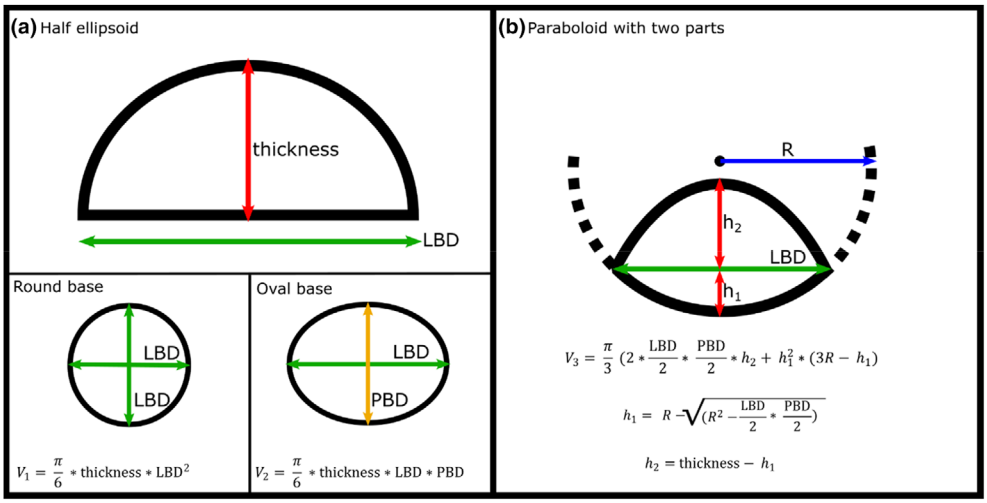

FIGURE 2 Models for calculation of uveal melanoma tumour volume. Thickness, LBD and PBD are determined automatically based on the MRI contours. (a) The two ellipsoid tumour models with their respective interpretations of the tumour base. (b) The paraboloid model with two parts. R: Eye radius, assumed to be 12 mm (Escudero-Sanz & Navarro, 1999); $h_1 = \sqrt{(R^2 - \text{LBD}/2 * \text{SBD}/2)}$; $h_2 = \text{thickness} - h_1$.

observers (LK and JWB), and disagreements were discussed in a consensus meeting.

2.3 | Tumour models

The volume of the delineated tumours was compared to the volume calculated with three frequently used tumour models, based on the thickness and basal diameters of the MRI delineation (Figure 2). The most straightforward model, the half ellipsoid with round base ($V_{roundbase}$), uses tumour thickness and largest basal diameter to approximate tumour volume. First used for prognosis by Richtig et al. (2004), this model is used for prognosis, growth rate estimation and treatment response assessment (Augsburger et al., 1984; Gillam et al., 2023; Singh, 2001; Uner et al., 2021).

Other studies propose a half ellipsoid with an oval base ($V_{ovalbase}$). This model uses both the largest basal diameter and the perpendicular basal diameter, and is used for prognosis and treatment planning comparisons (Char et al., 1997; Furdova et al., 2018, 2022; Gass, 1985; Studenski et al., 2020; Tien et al., 2017).

The most extensive model compared in this study is the paraboloid with two parts ($V_{twoparts}$). This model assumes the tumour consists of a paraboloid, comparable to the half ellipsoid in the previously mentioned formulas, and a spherical cap approximating the curvature of the eye. Variations of this model are applied in the context of comparison with new treatment planning and diagnostic techniques (Caminal et al., 2016; Daftari et al., 2005) and prognosis (Li et al., 2003). The model compared in this study was proposed by Caminal et al. (2016). In this study, the radius of the eye was assumed to be 12 mm (Escudero-Sanz & Navarro, 1999).

2.4 | Statistics

All three tumour models were compared with the MRI-delineated tumour volume. Mean differences and mean absolute differences were determined. Model volumes were compared with the MRI-delineated tumour volume using two-tailed paired t-tests or Wilcoxon signed-rank tests, depending on the results of the Shapiro-Wilks test for normality. This analysis was repeated for all three models and for the group before treatment, the group after treatment and the entire cohort, resulting in 9 comparisons. Therefore, the significance level was adjusted using a Bonferroni correction, resulting in a significance level of $p < 0.0056$.

To assess whether tumour shape influenced the difference between the MRI-delineated and estimated tumour volume, the difference between the regular and irregular tumour shapes was determined in a multiple linear regression, also taking tumour volume into account.

3 | RESULTS

From the retrospective cohort, 60 patients were assessed for the inclusion and exclusion criteria. Four patients were excluded: 1 had extrascleral extensions and 3 were evaluated to assess possible tumour recurrences. One patient underwent endoresection between the pre-treatment and post-treatment scan, and therefore, the post-treatment scan was excluded from this study.

Including 14 patients of the prospective cohort, in total 70 patients were included in this study. For 35/70 patients, both pre-treatment and post-treatment scans were available, resulting in 105 scans. The majority received proton beam therapy (64%), while 23% received brachytherapy and 11% underwent enucleation.

3.1 | Before treatment

Average (± standard deviation) tumour volume on MRI before treatment was 567 ± 415 mm^3 (range 33–1663 mm^3). Average thickness, LBD and PBD were 6.4 ± 3.0 mm (range 1.3–12.9 mm), 15.0 ± 3.7 mm (range 7.2–22.4 mm) and 12.5 ± 3.1 mm (range 6.0–20.9 mm), respectively. AJCC TNM staging (Kivelä et al., 2016) was as follows: T1: 13%, T2: 14%, T3: 50%, T4: 23%.

TABLE 1 Mean difference between tumour models and MRI volume.

Mean difference between tumour models and MRI-delineated volume ± SD (range)								
	Before treatment ($n=70$)			After treatment ($n=35$)			Entire cohort ($n=105$)		
	Volume [mm^3]	Relative [%]	*p*-value	Volume [mm^3]	Relative [%]	*p*-value	Volume [mm^3]	Relative [%]	*p*-value
$V_{roundbase}$	303 ± 254 (−52–975)	53 ± 30 (−18–129)	<0.001	265 ± 258 (−19–1070)	54 ± 35 (−28–133)	<0.001	291 ± 256 (−53–1070)	53 ± 32 (−29–133)	<0.001
$V_{ovalbase}$	163 ± 151 (−128–651)	28 ± 22 (−44–78)	<0.001	123 ± 124 (−27–433)	23 ± 29 (−45–108)	<0.001	150 ± 144 (−128–651)	26 ± 24 (−45–108)	<0.001
$V_{twoparts}$	101 ± 128 (−252–550)	16 ± 23 (−69–69)	<0.001	79 ± 99 (−41–351)	12 ± 27 (−50–92)	<0.001	94 ± 120 (−252–550)	15 ± 24 (−69–92)	<0.001

On average, all tumour models resulted in a significant overestimation of the tumour volume (Wilcoxon signed-rank tests, all $p<0.001$): the model volume was larger than the MRI-delineated volume in 97%, 89% and 84% for $V_{roundbase}$, $V_{ovalbase}$ and $V_{twoparts}$, respectively. Mean differences between the model and the MRI volume were smallest for the paraboloid model with two parts, which resulted in an average overestimation of 16 ± 23% ($V_{twoparts}$, Table 1). This model also resulted in the smallest variation in overestimation between patients. Between the two ellipsoid models, the model that incorporated the PBD ($V_{ovalbase}$) performed best, with an overestimation of 282 ± 22%. The largest differences between the model and the MRI tumour volume were observed for the ellipsoid with the round base ($V_{roundbase}$), with an average overestimation of 53 ± 30%, corresponding to the largest variation between patients. All differences between the tumour models and the MRI tumour volume are shown in Table 1 and Figure 3. An example of all three tumour models and the MRI delineation for tumours with a regular (dome) shape and an irregular (mushroom) shape is shown in Figure 4.

3.2 | After treatment

For the 35 patients with scans before and after treatment, average tumour volume did not change after treatment (511 ± 354 mm^3 versus 456 ± 409 mm^3, $p=0.07$). Tumour model performance was similar to the pre-treatment group (Table 1).

3.3 | Effect of tumour volume and shape

In a multiple linear regression, tumour volume and tumour shape did not have a statistically significant effect on the relative difference between the model volumes and MRI-delineated tumour volume for all tumour models (Table S1).

4 | DISCUSSION

Ellipsoid tumour models are used to determine uveal melanoma volume to estimate prognosis, to compare tumour volumes to other modalities and to perform treatment planning comparisons. In this study, we show that frequently used methods result in considerable systematic overestimations of the MRI-delineated tumour volume and large variation in overestimation between patients.

All tumour models resulted in systematic overestimations of the MRI-delineated tumour volume, which was smallest in the paraboloid with two parts (15%). This model also had the smallest variation between patients (SD: 24%), although it was comparable to the ellipsoid with oval base (SD: 24%), for which a larger mean overestimation was observed.

The paraboloid with two parts may be further improved by measuring the radius of the eye instead of taking a population average, as was done in this study. However,

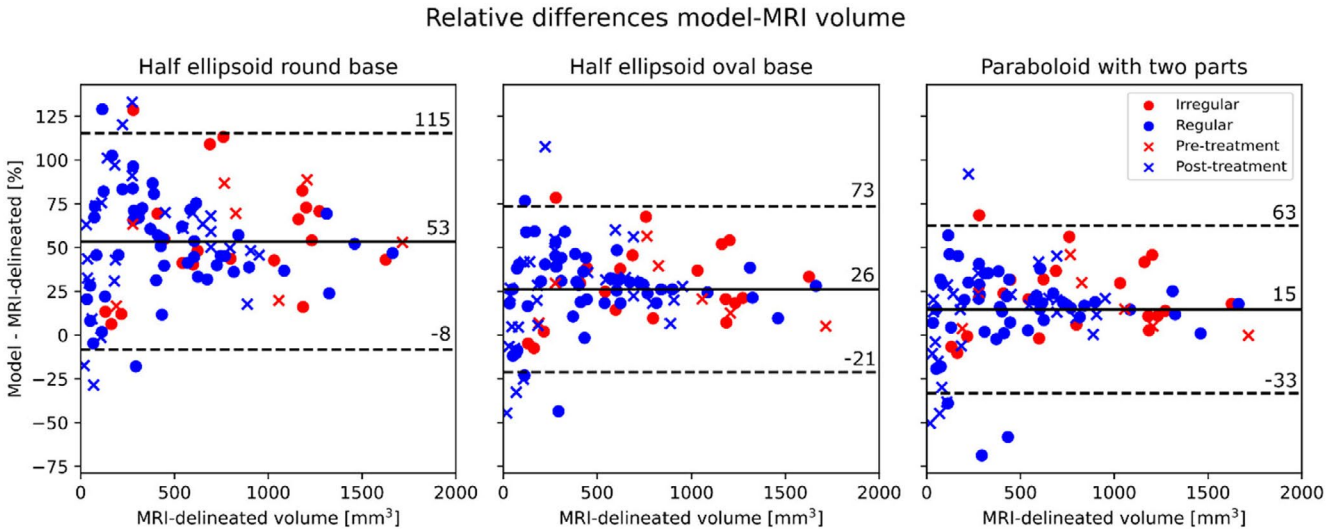

FIGURE 3 Differences between the calculated tumour volume with three tumour models and the MRI-delineated tumour volume. Mean (solid line) and confidence intervals (dashed line) are shown for the entire cohort.

decreasing or increasing the radius by 1 mm (Van Vught et al., 2021) resulted in a volume change of 0.5%, suggesting this improvement would have a limited effect. Furthermore, using a population average, this method can be used by only measuring the thickness and two basal diameters, making it easily applicable in routine clinical care and in retrospective studies. The half ellipsoid with a round base ($V_{roundbase}$) resulted in the largest overestimation and largest variation in overestimation within the cohort. An improvement of this model was proposed by Stalhammar et al. (2024), adjusting the perpendicular diameter to 85% of the largest basal diameter. Although in our cohort this proportion between the largest and perpendicular diameter was similar, this adjustment does not decrease the large variation between patients.

Although dome-shaped tumours are the most frequently occurring tumour shape, uveal melanoma may appear in several shapes, especially after breaking through Bruch's membrane (Ferreira et al., 2022; Foti et al., 2021). Although not significant, the effect of tumour shape was largest in the half ellipsoid with a round base and smallest in the paraboloid with two parts. Arnljots et al. (2018) used the second theorem of Pappus to estimate tumour volume by determining the surface area of two halves of enucleated tumours on histology slices, which might result in a more accurate volume estimation in enucleated eyes than the ellipsoid tumour models in this paper, especially for tumours with an irregular shape.

One previous study compared the MRI tumour volume with the half ellipsoid with oval base (Furdova et al., 2022). However, this study aimed to compare MRI and ultrasound tumour volume and therefore used the ultrasound measurements for the model, making it difficult to directly compare the results. However, in both this study and in our cohort, the model volume was larger than the MRI tumour volume. Although previous studies show that on average ultrasound measurements agree with MRI measurements, the latter are more accurate in anteriorly located tumours, especially if not the entire tumour extent is visible in the ultrasound images (Jaarsma-Coes, Klaassen, Marinkovic, et al., 2023). Therefore, using ultrasound measurements for tumour volume estimation would result in even more patient-specific variation.

More accurate estimations of tumour volume may contribute to improved prediction of metastasis and survival. Despite it being an important factor, frequently used models result in an overestimation of the tumour volume and the amount of overestimation varies significantly between patients. Here, systematic overestimations will likely not affect the accuracy of prognosis estimation, since patients with similarly sized tumours will remain equally sized. However, the large variation between patients will likely heavily influence the results. For example, two tumours from our cohort with a comparable volume on MRI of 1181 and 1185 mm^3 had model volumes of 2156 and 1375 mm^3 ($V_{roundbase}$). According to Stalhammar et al. (2024), who adjusted the ellipsoid with round base by a factor of 0.85, these two tumours would be categorized as V3 and V4, corresponding to an increase in hazard ratio of 2.32 for metastatic death. Similarly, the AJCC classification, which uses thickness and largest diameter to estimate prognosis (Force, 2015; Kivelä et al., 2016), might not be an optimal representation of tumour load. All in all, this shows that models using two or three tumour dimension measurements might offer valuable estimations on a group level, but show large differences on an individual level, and that therefore a more accurate determination of tumour volume might improve prognosis estimation.

Beside prognosis, ellipsoid tumour models are also used in treatment response assessment of uveal melanoma. In this study, we show that model performance is similar before and after treatment, although tumour volume often has not decreased in size at the time of the first follow-up MRI scan (Tang et al., 2023).

This study shows that using the best-performing tumour model decreases systematic errors in tumour volume estimation and halves the variation between patients. In the future, three-dimensional imaging may become more widely available, for example due to the increase in image-guided ocular radiotherapy (Hrbacek et al., 2016, 2024), resulting in precise measurements of tumour volume instead of estimations. We hypothesize

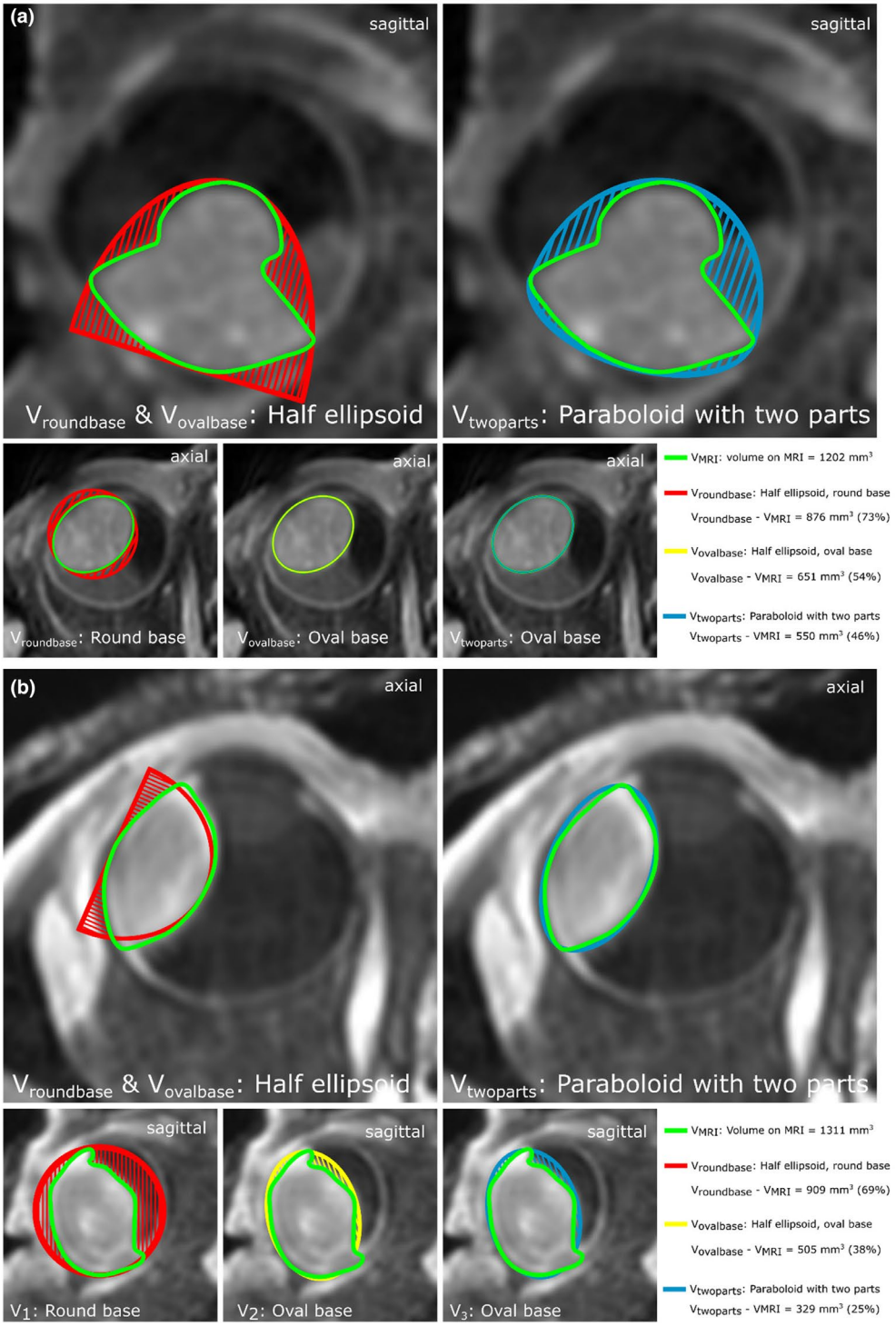

FIGURE 4 Two examples of the three tumour models and the MRI contours for patients with an irregular (mushroom) shape (a) and with a regular (dome) shape (b). Green: MRI tumour contours, red: Half ellipsoid with round base, yellow: Half ellipsoid with oval base, blue: Paraboloid with two parts.

that using delineated tumour volume as a prognostic tool may improve prognosis estimation, similar to other tumour sites (Duran et al., 2023; Studer et al., 2007; Thoenissen et al., 2024). However, future analyses using survival data in larger cohorts should be performed.

4.1 | Limitations

Due to the retrospective design of this study, a bias might exist towards larger tumours, as in our centre, these patients undergo standard MR exams to prepare for proton therapy, whereas patients with smaller tumours do not. Therefore, the number of patients receiving proton beam therapy in this cohort is larger than on average in our centre.

In this study, we assessed how well ellipsoid models can describe volume for uveal melanomas, which typically do not all have an ellipsoidal configuration. In this context, we used a three-dimensional delineation of the tumour, based on MR-images, as ground truth volume. We acknowledge that this method has its limitations, as flat extensions might be missed (Foti et al., 2021; Jaarsma-Coes, Klaassen, Marinkovic, et al., 2023). Nevertheless, earlier

studies showed that MRI provides a geometrically accurate representation of the tumour (Klaassen et al., 2024), and that MR-based prominence and basal diameter measures typically correspond well with ultrasound measurements (Jaarsma-Coes, Klaassen, Marinkovic, et al., 2023; Klaassen et al., 2022), upon which most current staging methods, such as the AJCC classification, are mostly based (Shields et al., 2015). Future improvements in MRI delineations may be achieved by combining MRI with optical methods such as fundoscopy (Haasjes et al., 2024), which may aid in accurately including thin lesions and flat tumour extensions. This is particularly relevant for 9 out of 70 patients in this study with a flat lesion of which the tumour extent was more difficult to assess on MRI. However, as the tumour model was based on the dimensions of the MRI delineation, slight inaccuracies in delineation would influence both the MRI-delineated volume and the tumour model in the same way and therefore not impact the reported differences.

5 | CONCLUSION

All ellipsoid tumour models result in considerable systematic overestimations of tumour volume, with large variations in overestimation between patients. Adding the perpendicular basal diameter to the model decreases the variation between patients. Although ellipsoid tumour models have been shown to be valuable on a group level, they should be used with caution on an individual level.

FUNDING INFORMATION

This research was funded by Varian, a Siemens Healthineers company (HollandPTC-Varian Consortium grant ID (project 2020016)). They had no role in the study design, the collection, analysis or interpretation of data, and the writing of the report.

The C.J. Gorter MRI Centre, to which LK and JWB are affiliated, receives research support from Philips Healthcare.

ORCID

Lisa Klaassen https://orcid.org/0000-0001-9874-7206

REFERENCES

Arnljots, T.S., AL-Sharbaty, Z., Lardner, E., All-Eriksson, C., Seregard, S. & Stalhammar, G. (2018) Tumour thickness, diameter, area or volume? The prognostic significance of conventional versus digital image analysis-based size estimation methods in uveal melanoma. *Acta Ophthalmologica*, 96, 510–518.

Augsburger, J.J., Gonder, J.R., Amsel, J., Shields, J.A. & Donoso, L.A. (1984) Growth rates and doubling times of posterior uveal melanomas. *Ophthalmology*, 91, 1709–1715.

Buonanno, F., Conson, M., De Almeida Ribeiro, C., Oliviero, C., Itta, F., Liuzzi, R. et al. (2022) Local tumor control and treatment related toxicity after plaque brachytherapy for uveal melanoma: A systematic review and a data pooled analysis. *Radiotherapy and Oncology*, 166, 15–25.

Caminal, J.M., Mejia, K., Arias, L., Masuet-Aumatell, C., Larruceа-Maseda, J., Modolell, I. et al. (2016) Tumor volumes in choroidal melanoma: Agreement between three-dimensional ultrasound and two mathematical models. *American Journal of Ophthalmology*, 166, 181–188.

Char, D.H., Kroll, S. & Phillips, T.L. (1997) Uveal melanoma. Growth rate and prognosis. *Archives of Ophthalmology*, 115, 1014–1018.

Daftari, I., Aghaian, E., O'Brien, J.M., Dillon, W. & Phillips, T.L. (2005) 3D MRI-based tumor delineation of ocular melanoma and its comparison with conventional techniques. *Medical Physics*, 32, 3355–3362.

Duran, A.O., Inanc, M., Bozkurt, O., Ozaslan, E. & Ozkan, M. (2023) Tumor volume is a better prognostic factor than greatest tumor diameter in operated stage I-III non-small-cell lung cancer. *Clinical Lung Cancer*, 24, 252–259.

Escudero-Sanz, I. & Navarro, R. (1999) Off-axis aberrations of a wide-angle schematic eye model. *Journal of the Optical Society of America. A, Optics, Image Science, and Vision*, 16, 1881–1891.

Ferreira, T.A., Grech Fonk, L., Jaarsma-Coes, M.G., Van Haren, G.G.R., Marinkovic, M. & Beenakker, J.M. (2019) MRI of uveal melanoma. *Cancers (Basel)*, 11, 377.

Ferreira, T.A., Jaarsma-Coes, M.G., Marinkovic, M., Verbist, B., Verdijk, R.M., Jager, M.J. et al. (2022) MR imaging characteristics of uveal melanoma with histopathological validation. *Neuroradiology*, 64, 171–184.

Force, A.O.O.T. (2015) International validation of the American joint committee on Cancer's 7th edition classification of uveal melanoma. *JAMA Ophthalmology*, 133, 376–383.

Foti, P.V., Travali, M., Farina, R., Palmucci, S., Spatola, C., Raffaele, L. et al. (2021) Diagnostic methods and therapeutic options of uveal melanoma with emphasis on MR imaging-part I: MR imaging with pathologic correlation and technical considerations. *Insights Into Imaging*, 12, 66.

Furdova, A., Babal, P., Kobzova, D., Zahorjanova, P., Kapitanova, K., Sramka, M. et al. (2018) Uveal melanoma survival rates after single dose stereotactic radiosurgery. *Neoplasma*, 65, 965–971.

Furdova, A., Furda, R., Sramka, M., Chorvath, M., Rybar, J., Vesely, P. et al. (2022) Stereotactic irradiation on linear accelerator – Ultrasound versus MRI in choroidal melanoma volume calculation. *BMC Ophthalmology*, 22, 333.

Gass, J.D. (1985) Comparison of prognosis after enucleation vs cobalt 60 irradiation of melanomas. *Archives of Ophthalmology*, 103, 916–923.

Gillam, M., Fenech, G.A., Chadwick, O., Nairn, J., Chadha, V., Connolly, J. et al. (2023) When is the optimum radiological response to proton beam therapy in uveal melanoma? *Ocular Oncology and Pathology*, 9, 130–137.

Haasjes, C., Vu, T.H.K. & Beenakker, J.M. (2024) Patient-specific mapping of fundus photographs to three-dimensional ocular imaging. *Medical Physics*. Available from: https://doi.org/10.1002/mp.17576

Hagstrom, A., Witzenhausen, H. & Stalhammar, G. (2024) Tailoring surveillance imaging in uveal melanoma based on individual metastatic risk. *Canadian Journal of Ophthalmology*, 60, e240–e252.

Hou, X., Rokohl, A.C., Li, X., Guo, Y., Ju, X., Fan, W. et al. (2024) Global incidence and prevalence in uveal melanoma. *Advances in Ophthalmology Practice and Research*, 4, 226–232.

Hrbacek, J., Kacperek, A., Beenaker, J.M., Mortimer, L., Denker, A., Mazal, A. et al. (2024) PTCOG ocular statement: expert summary of current practices and future developments in ocular proton therapy. *International Journal of Radiation Oncology, Biology, Physics*, 120, 1307–1325.

Hrbacek, J., Mishra, K.K., Kacperek, A., Dendale, R., Nauraye, C., Auger, M. et al. (2016) Practice patterns analysis of ocular proton therapy centers: the international OPTIC survey. *International Journal of Radiation Oncology, Biology, Physics*, 95, 336–343.

Jaarsma-Coes, M.G., Ferreira, T.A., Marinkovic, M., Vu, T.H.K., Van Vught, L., Van Haren, G.R. et al. (2023) Comparison of magnetic resonance imaging-based and conventional measurements for proton beam therapy of uveal melanoma. *Ophthalmol Retina*, 7, 178–188.

Jaarsma-Coes, M.G., Klaassen, L., Marinkovic, M., Luyten, G.P.M., Vu, T.H.K., Ferreira, T.A. et al. (2023) Magnetic resonance imaging in the clinical care for uveal melanoma patients-a systematic review from an ophthalmic Perspective. *Cancers (Basel)*, 15, 2995.

Jaarsma-Coes, M.G., Klaassen, L., Verbist, B.M., Vu, T.H.K., Klaver, Y.L.B., Rodrigues, M.F. et al. (2023) Inter-observer variability

in MR-based target volume delineation of uveal melanoma. *Advances in Radiation Oncology*, 8, 101149.
Jager, M.J., Shields, C.L., Cebulla, C.M., Abdel-Rahman, M.H., Grossniklaus, H.E., Stern, M.H. et al. (2020) Uveal melanoma. *Nature Reviews Disease Primers*, 6, 24.
Kaliki, S., Shields, C.L. & Shields, J.A. (2015) Uveal melanoma: estimating prognosis. *Indian Journal of Ophthalmology*, 63, 93–102.
Kivelä, T., Simpson, R.E., Grossniklaus, H.E. & Al, E. (2016) *Uveal melanoma. AJCC cancer staging manual*, 8th edition. New York, NY: Springer.
Klaassen, L., Haasjes, C., Hol, M., Cambraia Lopes, P., Spruijt, K., Van De Steeg-Henzen, C. et al. (2024) Geometrical accuracy of magnetic resonance imaging for ocular proton therapy planning. *Physics and Imaging in Radiation Oncology*, 31, 100598.
Klaassen, L., Jaarsma-Coes, M.G., Verbist, B.M., Vu, T.H.K., Marinkovic, M., Rasch, C.R.N. et al. (2022) Automatic three-dimensional magnetic resonance-based measurements of tumour prominence and basal diameter for treatment planning of uveal melanoma. *Physics and Imaging in Radiation Oncology*, 24, 102–110.
Kujala, E., Makitie, T. & Kivela, T. (2003) Very long-term prognosis of patients with malignant uveal melanoma. *Investigative Ophthalmology & Visual Science*, 44, 4651–4659.
Li, W., Gragoudas, E.S. & Egan, K.M. (2003) Tumor basal area and metastatic death after proton beam irradiation for choroidal melanoma. *Archives of Ophthalmology*, 121, 68–72.
Marinkovic, M., Horeweg, N., Fiocco, M., Peters, F.P., Sommers, L.W., Laman, M.S. et al. (2016) Ruthenium-106 brachytherapy for choroidal melanoma without transpupillary thermotherapy: similar efficacy with improved visual outcome. *European Journal of Cancer*, 68, 106–113.
Marinkovic, M., Pors, L.J., Van Den Berg, V., Peters, F.P., Schalenbourg, A., Zografos, L. et al. (2021) Clinical outcomes after international referral of uveal melanoma patients for proton therapy. *Cancers (Basel)*, 13, 6241.
Mishra, K.K. & Daftari, I.K. (2016) Proton therapy for the management of uveal melanoma and other ocular tumors. *Chinese Clinical Oncology*, 5, 50.
Richtig, E., Langmann, G., Mullner, K., Richtig, G. & Smolle, J. (2004) Calculated tumour volume as a prognostic parameter for survival in choroidal melanomas. *Eye (London, England)*, 18, 619–623.
Shields, C.L., Furuta, M., Thangappan, A., Nagori, S., Mashayekhi, A., Lally, D.R. et al. (2009) Metastasis of uveal melanoma millimeter-by-millimeter in 8033 consecutive eyes. *Archives of Ophthalmology*, 127, 989–998.
Shields, C.L., Kaliki, S., Furuta, M., Fulco, E., Alarcon, C. & Shields, J.A. (2015) American joint committee on cancer classification of uveal melanoma (anatomic stage) predicts prognosis in 7,731 patients: the 2013 Zimmerman lecture. *Ophthalmology*, 122, 1180–1186.
Singh, A.D. (2001) Uveal melanoma: implications of tumor doubling time. *Ophthalmology*, 108, 829–831.
Solnik, M., Paduszynska, N., Czarnecka, A.M., Synoradzki, K.J., Yousef, Y.A., Choragiewicz, T. et al. (2022) Imaging of uveal melanoma-current standard and methods in development. *Cancers (Basel)*, 14, 3147.
Stalhammar, G., Coupland, S.E., Ewens, K.G., Ganguly, A., Heimann, H., Shields, C.L. et al. (2024) Improved staging of ciliary body and choroidal melanomas based on estimation of tumor volume and competing risk analyses. *Ophthalmology*, 131, 478–491.
Studenski, M.T., Patel, N.V., Markoe, A., Harbour, J.W. & Samuels, S.E. (2020) Influence of tumor shape and location in eye plaque brachytherapy dosimetry. *Brachytherapy*, 19, 249–254.
Studer, G., Lutolf, U.M., EL-Bassiouni, M., Rousson, V. & Glanzmann, C. (2007) Volumetric staging (VS) is superior to TNM and AJCC staging in predicting outcome of head and neck cancer treated with IMRT. *Acta Oncologica*, 46, 386–394.
Tang, M.C.Y., Ferreira, T.A., Marinkovic, M., Jaarsma-Coes, M.G., Klaassen, L., Vu, T.H.K. et al. (2023) MR-based follow-up after brachytherapy and proton beam therapy in uveal melanoma. *Neuroradiology*, 65, 1271–1285.
Thoenissen, P., Engelmann, T., Heselich, A., Winkelmann, R., Burck, I., Sader, R. et al. (2024) MRI tumour volumetry as a new staging tool in diagnosis and therapy of oral cancer. *Journal of Cranio-Maxillo-Facial Surgery*, 52, 1140–1147.
Tien, C.J., Astrahan, M.A., Kim, J.M., Materin, M., Chen, Z., Nath, R. et al. (2017) Incorporating patient-specific CT-based ophthalmic anatomy in modeling iodine-125 eye plaque brachytherapy dose distributions. *Brachytherapy*, 16, 1057–1064.
Uner, O.E., See, T.R.O., Szalai, E., Grossniklaus, H.E. & Stalhammar, G. (2021) Estimation of the timing of BAP1 mutation in uveal melanoma progression. *Scientific Reports*, 11, 8923.
Van Vught, L., Shamonin, D.P., Luyten, G.P.M., Stoel, B.C. & Beenakker, J.M. (2021) MRI-based 3D retinal shape determination. *BMJ Open Ophthalmology*, 6, e000855.
Wu, M., Yavuzyigitoglu, S., Brosens, E., Ramdas, W.D., Kilic, E. & ROTTERDAM OCULAR MELANOMA Study, G. (2023) Worldwide incidence of ocular melanoma and correlation with pigmentation-related risk factors. *Investigative Ophthalmology & Visual Science*, 64, 45.

SUPPORTING INFORMATION

Additional supporting information can be found online in the Supporting Information section at the end of this article.

How to cite this article: Klaassen, L., Ferreira, T.A., Luyten, G. & Beenakker, J.-W. (2025) Estimating uveal melanoma volume with ellipsoid tumour models. *Acta Ophthalmologica*, 103, 691–698. Available from: https://doi.org/10.1111/aos.17492